

XAFS studies of nitrogenase: the MoFe and VFe proteins and the use of crystallographic coordinates in three-dimensional EXAFS data analysis

Richard W. Strange,^{a*} Robert R. Eady,^b
David Lawson^b and S. Samar Hasnain^a

^aMolecular Biophysics Group, CCLRC Daresbury Laboratory, Warrington, Cheshire WA4 4AD, UK, and ^bDepartment of Biological Chemistry, John Innes Centre, Norwich NR4 7UH, UK. E-mail: r.w.strange@dl.ac.uk

This paper reports a three-dimensional EXAFS refinement of the Mo coordination sphere of the FeMoco cluster of the dithionite-reduced MoFe protein from *Klebsiella pneumoniae* nitrogenase (Kp1) using the 1.6 Å-resolution crystallographic coordinates. At this resolution, the positions of the heavy (Fe and S) atoms of the cluster are well determined and there is excellent agreement between the crystallographic and EXAFS models. However, the lighter homocitrate and histidine ligands are poorly determined in the crystal structure, and it is shown that the application of EXAFS-derived distance restraints during the early stages of crystallographic refinement provides a means of substantially improving (by ~0.1 Å) the final crystallographic model. The consistency of the EXAFS analysis with the crystallographic information in this case justifies applications of EXAFS to cases where protein crystal structures are absent. Thus, the VFe protein of V-nitrogenase has been shown by EXAFS to possess a V-atom site catalytically similar to the well characterized MoFe-nitrogenases, with V replacing Mo.

Keywords: EXAFS; nitrogen fixation; nitrogenase; crystal structure; FeMoco.

1. Introduction

Nitrogenase, the enzyme responsible for biological nitrogen fixation, catalyses the ATP-dependent reduction of N₂ to ammonia (Burgess & Lowe, 1996; Howard & Rees, 1994). Nitrogenase is found in relatively few groups of bacteria but is responsible for the global cycling of some 10⁸ tonnes of N per year. All N₂-fixing organisms have a highly conserved nitrogenase system based on Mo and Fe, but some organisms additionally have alternative nitrogenases based on V and Fe, or on Fe alone (see Eady, 1996). The three nitrogenase systems, although clearly related, are genetically distinct and do not simply arise from the substitution of different metals into the same polypeptides. All three classes of nitrogenase are two-component metalloenzyme systems. The Mo-independent nitrogenases were discovered some 16 years ago and have not been as extensively studied as the Mo system, to which they are clearly related. V-nitrogenase and Fe-only-nitrogenase have a VFe protein and an FeFe protein, respectively, and an associated Fe protein. The structural genes for the three systems have been cloned and sequenced and, as shown in Fig. 1, have a high degree of homology. A comparison of the amino-acid sequences of the MoFe, VFe and FeFe proteins revealed that the amino-acid residues of the α and β subunits, which are ligands to the P clusters and FeMoco and which are invariant in all MoFe proteins known, are all also conserved in the other nitrogenases. This result, together with genetic data, which indicate that some of the genes involved in the biosynthesis of

FeMoco are required for functional V- and Fe-nitrogenases, provided strong presumptive evidence that they would also contain analogous cofactor centres to FeMoco. These similarities suggest a common mechanism for the activation and reduction of N₂. If this is the case, then only the Fe and possibly the S atoms of the cofactor centres can be involved in substrate binding. The role of the hetero-metal (Mo or V) would be in modulating the reactivity of the centre, as is observed in model chemical systems (Evans *et al.*, 1999). However, work on the Fe-only-nitrogenase, particularly X-ray absorption spectroscopy, has been hindered by the lack of a hetero-metal in this system.

2. Experimental

EXAFS measurements were carried out at the Synchrotron Radiation Source, Daresbury Laboratory, operating at 2 GeV and an average current of 200 mA. Mo *K*-edge spectra were taken on the 5 T Wiggler station (9.2). A double-crystal Si(220) monochromator was employed with the crystals offset to give 50% of the maximum intensity. This arrangement allows harmonic content level < 0.1%. Data were measured in fluorescence mode using a Canberra 13-element Ge solid-state detector. The detector was calibrated using the Mo *K* α fluorescence signals from a 5 mM sample of molybdate. V *K*-edge data were measured on station 8.1 using a similar fluorescence detector. All measurements were made with samples in a liquid-nitrogen cryostat. Several 1 h scans of each sample were taken and then summed together after examining the output of each detector element. Normalization and background subtraction of the summed data were carried out by standard methods, as previously described. Analysis of the background-subtracted *k*³-weighted raw

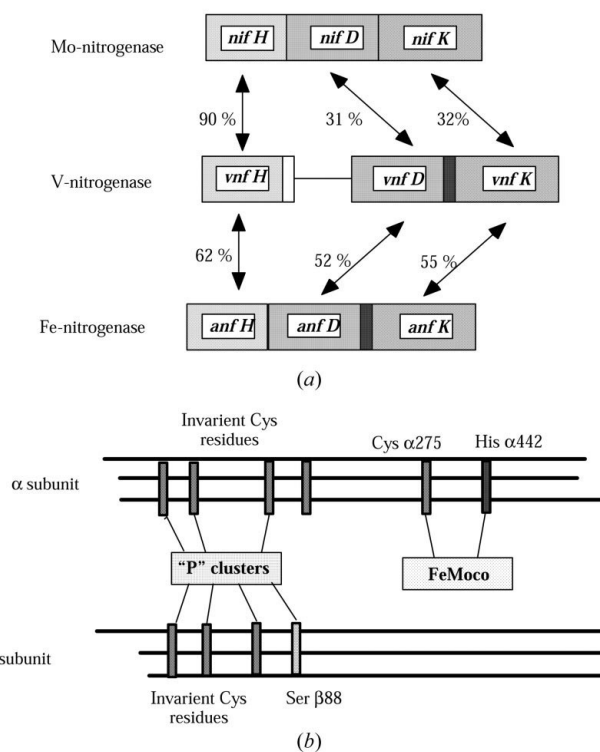


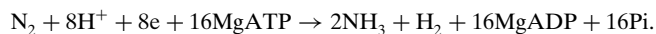
Figure 1
(a) Organization of the structural genes of the three nitrogenase systems showing the percentage of identical residues. (b) Comparison of the conserved residues of the α and β subunits of the three nitrogenases showing the ligands involved in the 'P' cluster and FeMoco binding in the MoFe proteins.

EXAFS was performed with the *EXCURV98* program (Binsted & Hasnain, 1996) using fast curved wave theory (Gurman *et al.*, 1984). The phase shifts employed were calculated using Hedin–Lundqvist exchange and correlation potentials.

3. Results and discussion

3.1. Mo-nitrogenases

The molybdenum-containing nitrogenase systems are composed of two metalloproteins: the MoFe protein (component 1) and the Fe protein (component 2). One role of the Fe protein is to act as a very specific MgATP-dependent electron donor to the MoFe protein to catalyse the reaction



The MoFe protein contains two unique metallosulfur clusters, *viz.* the P clusters and the FeMo cofactor centres (FeMoco). The 8Fe7S P clusters are probably the site of initial acceptance of electrons from the Fe protein. The FeMoco centres constitute the substrate binding and reducing sites of the MoFe protein and can be described as [MoFe₃S₃] and [Fe₄S₃] clusters linked by three S²⁻ bridges. The Mo atom is also coordinated to homocitrate *via* hydroxyl and carboxyl O atoms (Fig. 2). Structural characteristics of the FeMoco centre were first provided by EXAFS (Arber *et al.*, 1988; Cramer *et al.*, 1978) and subsequently confirmed by several crystal structures of MoFe proteins (Bolin *et al.*, 1990; Chan *et al.*, 1993; Georgiadis *et al.*, 1992; Kim & Rees, 1992; Kim *et al.*, 1993; Mayer *et al.*, 1999). The resolution of these crystal structures has been improved with time but is still far from ‘atomic’ (< 1.2 Å). In this paper we report a three-dimensional EXAFS refinement (Cheung *et al.*, 2000) using the 1.6 Å-resolution crystallographic coordinates (PDB code 1QGU) for the dithionite-reduced MoFe protein from *Klebsiella pneumoniae* nitrogenase (Kp1) (Mayer *et al.*, 1999). The results show a good agreement for interatomic distances for most of the cluster atoms except for the low-Z ligands. The application of EXAFS-derived distance restraints during the early stages of crystallographic refinement provides a means of substantially improving (by ~0.1 Å) the agreement with the final model.

The asymmetric unit of Kp1 contains an $\alpha_2\beta_2$ tetramer with the $\alpha\beta$ halves related by a non-crystallographic twofold axis, and each $\alpha\beta$ dimer contains one FeMoco centre and one P cluster, giving two independent measurements for each interatomic distance. These two sets of measurements were essentially identical (within ± 0.04 Å in the worse case) at 1.6 Å resolution (Mayer *et al.*, 1999). For the EXAFS calculations, the atomic coordinates for a single FeMoco site (Fig. 2) were used without averaging. Table 1 summarizes the details of the interatomic distances for a three-dimensional constrained refinement of the EXAFS where only the Debye–Waller factors (σ^2) were allowed to refine and the distances were fixed at crystallographic values. Also included are the fit parameters obtained from a three-dimensional constrained refinement where interatomic distances were also allowed to change. The two simulations are shown in Fig. 3. In the first refinement, the σ^2 values of the low-Z atoms have increased to the extent that these atoms no longer make any contribution to the EXAFS spectrum, which establishes that their distances are incorrect. In the second refinement, with more reasonable σ^2 terms, these atoms shift significantly; the imidazole N atom moves by ~0.2 Å while the O atoms of the homocitrate are rotated to give a change in distance of ~0.1 Å. At the same time, there is little difference between the two refinements for the rest of the cluster: the Mo–S and Mo–Fe distances are within 0.01 Å of their crystallographic values, including the Mo–Fe shell at ~5 Å.

Table 1

Constrained refinements of the Mo *K*-edge EXAFS using a three-dimensional refinement approach.

In the first refinement, distances are kept at crystallographic values and Debye–Waller (σ^2) values are refined; in the second refinement, the distances are also allowed to vary. A higher value than 0.03 Å² signifies that the atom is incorrectly placed and that little contribution to the EXAFS signal is made. ΔR is the difference in Mo–ligand distance from the crystallographic value averaged over the two independent $\alpha\beta$ units.

Ligand	First refinement		Second refinement		ΔR (Å)
	<i>R</i> (Å)	σ^2 (Å ²)	<i>R</i> (Å)	σ^2 (Å ²)	
Mo–N(His)	2.48	0.11	2.29	0.003	–0.17
Mo–O5(homocitrate)	2.29	0.11	2.14	0.001	–0.16
Mo–O7(homocitrate)	2.35	0.11	2.31	0.001	–0.04
Mo–S1B	2.30	0.001	2.30	0.001	0.0
Mo–S3B	2.38	0.001	2.37	0.001	–0.01
Mo–S4B	2.35	0.001	2.35	0.001	0.00
Mo–Fe7	2.67	0.006	2.67	0.006	0.00
Mo–Fe6	2.68	0.006	2.67	0.006	–0.01
Mo–Fe5	2.71	0.006	2.71	0.006	0.00
Mo–Fe2	5.04	0.01	5.04	0.01	0.00
Mo–Fe3	5.06	0.01	5.06	0.01	0.00
Mo–Fe4	5.09	0.01	5.08	0.01	–0.01
Fit index		12.4		9.5	
<i>R</i> factor	46%		37%		

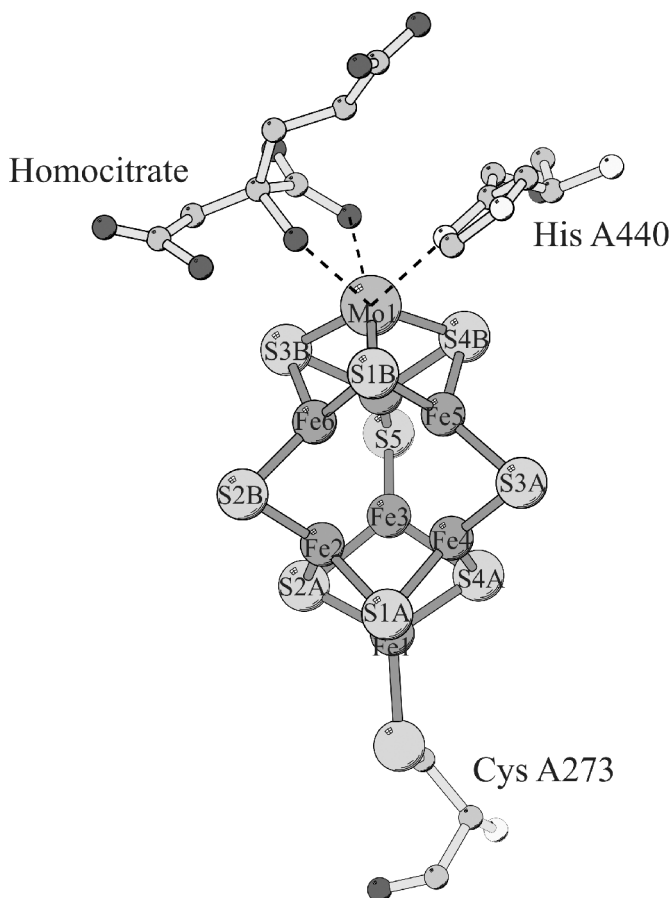


Figure 2
Structure of FeMoco site in Kp1 nitrogenase.

Thus, the agreement between the PX and EXAFS structures regarding the positions of the heavier, more strongly scattering atoms is better than that for the light atoms.

A similar observation has been made for the type-1 copper proteins, like azurins, where the Cu–S(Cysteine) distance is essentially the same by PX and EXAFS (*i.e.* within ± 0.02 Å) but the low-Z histidine ligands are found to differ by ~ 0.1 Å in their distances to the Cu atom, the values from PX being consistently longer (Cheung *et al.*, 2000; Dodd *et al.*, 2000; Murphy *et al.*, 1993). On the other hand, there is no such discrepancy regarding the comparison between small-molecule crystallography and EXAFS, where the distances of light- and heavy-scattering atoms are normally determined to within ± 0.02 Å of each other, for example, the Mo–O and Mo–S distances in $[\text{Nbu}_4^+]_2[\text{MoO}(\text{mnt})_2]$ (Baugh *et al.*, 1997). The Cambridge Structural Database (Allen & Kennard, 1993) yields six small-molecule structures relevant to the octahedral Mo coordination in FeMoco. These structures have average Mo–S bond lengths in agreement with the XAFS and PX results for Kp1 [2.36 (0.02) Å]. On the other hand, the average Mo–O [2.13 (0.04) Å] and Mo–N [2.28 (0.01) Å] bond lengths agree closely with the EXAFS results for Kp1. This agreement suggests that the distances are more accurately determined by EXAFS than by crystallography, at least at resolutions of ~ 1.6 Å.

Fitting the measured electron density by refining the structure using the EXAFS distances from the second refinement in Table 1 caused some distortion of the imidazole ring of the histidine residue. Consequently, we attempted a series of refinement protocols in order to try to reconcile the PX and EXAFS data (see Table 2). The coordinates from 1QGU were crudely randomized by applying a shift of $+0.1$ Å to one coordinate (*i.e.* *x* of atom 1) and -0.1 Å to the next (*i.e.* *y* of atom 1) and so on, alternating between $+0.1$ Å and -0.1 Å throughout the whole PDB file. Also, the temperature factors were all reset to 15 Å² (the value from *TRUNCATE* was 14.8 Å²). This model was then subjected to restrained refinement in *REFMAC*

Table 2

A summary of nearest Mo–ligand distances following *REFMAC* restrained-refinement protocols using XAFS restraints.

The final R_{free} values were 20% for each run (and 19.9% for 1QGU) with DPI based on R_{free} of 0.09 Å. The matrix value in the *REFMAC* refinements was 0.9 except for run 3 in which it was 0.5.

	XAFS restraints	Mo–N ⁸¹ (Å)	Mo–O5 (Å)	Mo–O7 (Å)
XAFS	–	2.29	2.14	2.31
1QGU	–	2.48 (0.02)	2.29 (0.01)	2.35 (0.00)
Run 1	Yes	2.34 (0.01)	2.20 (0.01)	2.28 (0.01)
Run 2	Yes	2.34 (0.02)	2.20 (0.01)	2.28 (0.01)
Run 3	Yes	2.33 (0.01)	2.19 (0.01)	2.29 (0.01)
Run 4	No	2.38 (0.02)	2.25 (0.02)	2.25 (0.01)
Run 5	No	2.38 (0.02)	2.25 (0.02)	2.25 (0.01)

(Murshudov *et al.*, 1997) with anisotropic temperature-factor refinement for the Mo atoms. For runs 2 to 4, the starting model was modified by placing the Mo atoms back at their final positions in 1QGU and the N⁸¹, O5 and O7 atoms at the EXAFS distances away from them. Then these models were refined either with tight restraints to the EXAFS values (between the clusters and their ligands) or with these restraints effectively switched off. The resulting structure places the histidine ligand closer by ~ 0.1 Å to the EXAFS model. The homocitrate O atoms occupy equivalent distances from the Mo. This structure was used as the starting model for further EXAFS refinements. The fit index and *R* factor for the starting model were poor (13.4% and 47%); subsequently, the fit converged to the second refinement model shown in Table 1.

In protein crystallographic studies, which are typically carried out at ~ 2 Å resolution, the presence of a heavy metal causes significant series-termination effects in the electron-density maps at about the same position as the position of the ligating atoms. The size of this ripple from the heavy metal is very significant compared with the scattering from the low-Z atom (Schindelin *et al.*, 1997). The availability of higher-resolution crystallographic structures will help further clarify this aspect.

In the absence of atomic resolution (1.2 Å or better), a three-dimensional EXAFS refinement combined with a high-resolution structure (~ 2 Å) is a useful approach for obtaining highly precise stereochemical information. This is of particular importance when the effects of substrate binding or redox reactions are investigated and when subtle structural changes are expected to occur. An approach similar in spirit to the one described here was taken by Chen *et al.* (1993). They refined a model of the Cp1 FeMo-cofactor using single-crystal Mo and Fe EXAFS, although the major issues in their report were on positioning of the heavy atoms, whereas our emphasis is on positioning of the light atoms and the comparison between the cofactors in the MoFe and VFe proteins

3.2. V-nitrogenases

The VFe proteins from *Azotobacter vinelandii* (Av1^v) (Hales *et al.*, 1986) and *A. chroococcum* (Ac1^v) (Eady *et al.*, 1987) have been purified and characterized to

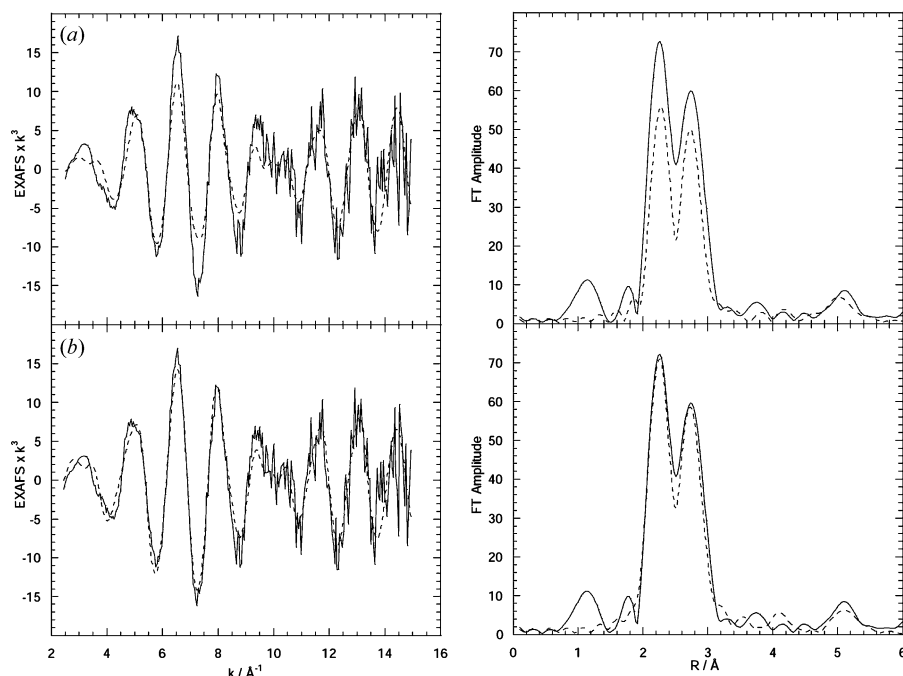


Figure 3
 k^3 -weighted EXAFS fits and corresponding Fourier transforms of reduced FeMoco (*a*) using 1.6 Å-resolution crystal structure coordinates and (*b*) after three-dimensional EXAFS refinement.

show that they generally have very similar properties. The focus of much of the work on these systems has been on the types of redox centres that are present in the proteins and how the presence of V changes the catalytic properties compared with Mo-nitrogenase. Electron paramagnetic resonance (EPR), magnetic circular dichroism (CD) and Mössbauer studies of these proteins are consistent with them containing P clusters and a cofactor centre analogous to FeMoco but containing V. These spectroscopic data fit well with the genetic and sequence data discussed above, which predict that such centres are present in VFe proteins (see Eady, 1996). Further supporting evidence for the presence of cofactor binding sites is provided by the ability of isolated FeMoco to bind and activate apo-Av1^V (Moore *et al.*, 1994).

The detail of the environment of V in these cofactor centres, in the absence of a crystal structure of a VFe protein, has been provided from EXAFS studies. The V EXAFS of Av1^V was initially compared with the model compound [Me₄N][VFe₃S₄Cl₃(DMF)₃]. This study, the first application of V K-edge X-ray absorption spectroscopy to a biological system, indicated that the V atom had a distorted octahedral symmetry and was in a similar environment to that in the model compound (Arber *et al.*, 1987). The data for Av1^V are very similar (George *et al.*, 1988), and the EXAFS region for both proteins can be simulated by a three-component fit with Fe, S and O as nearest neighbours to the V atom. This assignment and the distances of the atoms from the V atom are very similar to those for Mo in the FeMoco centre of MoFe proteins. In the case of MoFe proteins, the X-ray structure removed the ambiguity as to the nature of the light atoms; the Mo is coordinated to the carboxyl and hydroxyl groups of homocitrate and an N atom of the imidazole of His442. As discussed above, both homocitrate and the corresponding His residue are implicated in V-nitrogenase function, allowing a fairly safe assignment of the light atoms in the first coordination shell of the V atom.

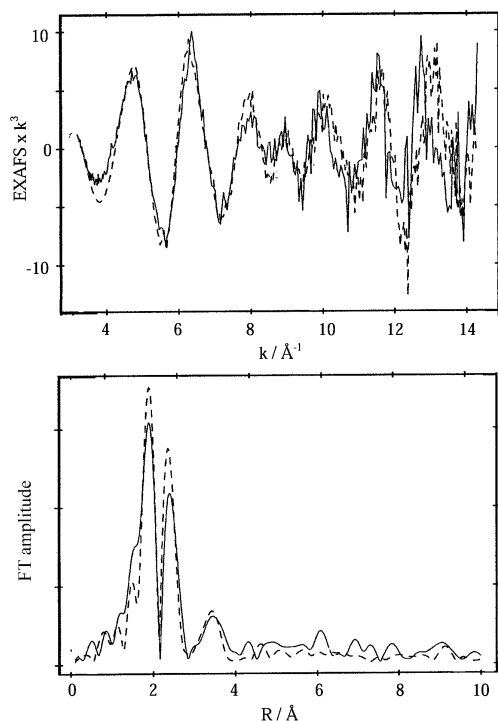


Figure 4
Comparison of Fe K-edge EXAFS data of FeVco (solid line) and FeMoco (dashed line).

Conditions were subsequently established that allowed the putative FeVco centres to be extracted into NMF in a form capable of activating MoFe apo-protein produced by mutant organisms defective in FeMoco biosynthesis (Smith *et al.*, 1988). The successful extraction of FeVco allowed the Fe EXAFS of the isolated cofactor to be determined and compared with the data for Av1^V (Harvey *et al.*, 1990). In this case, the EXAFS is dominated by Fe–S and Fe–Fe interactions at 2.32 and 2.64 Å, respectively. A longer Fe–Fe distance at 3.7 Å is also required in the simulation in all three cases. Fig. 4 shows the close similarity of both the EXAFS data and the Fourier transforms of the two cofactors and emphasizes their structural similarity.

4. Conclusion

XAFS has played a key role in the structural characterization of the nitrogenase cofactors. For MoFe nitrogenases, the first structural information on FeMoco was provided by XAFS in 1978 and demonstrated the presence of a cubane-type cluster. The overall organization of this cluster was confirmed by the crystal structure in the early 1990s, with clear identification of the presence of the low-Z ligands, histidine and homocitrate. The three-dimensional refinement of the XAFS data has shown that, even though these ligands are clearly seen in the crystal structure, their metrical data at 1.6 Å resolution suffer from an ambiguity that probably arises from the presence of the heavy metal, Mo. This example demonstrates the interplay between the X-ray absorption and diffraction techniques. For medium (<1.5 Å) resolution structures, we recommend using metrical information derived from XAFS as soft restraints in crystallographic refinement.

This work was supported by the BBSRC as part of the competitive strategic grant to JIC. We would like to thank Professor Barry Smith for his enthusiastic help and advice during this project.

References

- Allen, F. H. & Kennard, O. (1993). *Chem. Des. Autom. News*, **8**, 130–137.
- Arber, J. M., Dobson, B. R., Eady, R. R., Stevens, P., Hasnain, S. S., Garner, C. D. & Smith, B. E. (1987). *Nature (London)*, **325**, 372–375.
- Arber, J. M., Flood, A. C., Garner, C. D., Gormal, C. A., Hasnain, S. S. & Smith, B. E. (1988). *Biochem. J.* **252**, 421–425.
- Baugh, P. E., Garner, C. D., Charnock, J. M., Collison, D., Davies, E. S., McAlpine, A. S., Bailey, S., Lane, I., Hanson, G. R. & McEwan, A. G. (1997). *J. Biol. Inorg. Chem.* **2**, 643–643.
- Binsted, N. & Hasnain, S. S. (1996). *J. Synchrotron Rad.* **3**, 185–196.
- Bolin, J. T., Ronco, A. E., Mortenson, L. E., Morgan, T. V., Williamson, M. & Xuong, N.-H. (1990). *Nitrogen Fixation: Achievements and Objectives*, edited by P. M. Gresshoff, L. E. Roth, G. Stacey & W. E. Newton, pp. 117–121. New York/London: Chapman and Hall.
- Burgess, B. K. & Lowe, D. J. (1996). *Chem. Rev.* **96**, 2983–3011.
- Chan, K., Jim, J. & Rees, D. C. (1993). *Science*, **260**, 792–794.
- Chen, J., Christiansen, J., Campobasso, N., Bolin, J. T., Tittsworth, R. C., Hales, B., Rehr, J. & Cramer, S. P. (1993). *Angew. Chem. Int. Ed. Eng.* **32**, 1592–1594.
- Cheung, K. C., Strange, R. W. & Hasnain, S. S. (2000). *Acta Cryst.* **D56**, 697–704.
- Cramer, S. P., Hodgson, K. O., Gillum, W. O. & Mortensen, L. E. (1978). *J. Am. Chem. Soc.* **100**, 3398–3407.
- Dodd, F. E., Abraham, Z. H. L., Eady, R. R. & Hasnain, S. S. (2000). *Acta Cryst.* **D56**, 690–696.
- Eady, R. R. (1996). *Chem. Rev.* **96**, 3013–3030.
- Eady, R. R., Robson, R. L., Richardson, T. H., Miller, R. W. & Hawkins, M. (1987). *Biochem. J.* **244**, 197.
- Evans, D. J., Henderson, R. A. & Smith, B. E. (1999). *Bioinorganic Catalysis*, edited by J. Reedijk & E. Bouwman, pp. 153–207. New York: Marcel Dekker.

- George, G. N., Coyle, C. L., Hales, B. J. & Cramer, S. P. (1988). *J. Am. Chem. Soc.* **110**, 4057–4059.
- Georgiadis, M. M., Komiya, H., Chakrabarti, P., Woo, D., Kornuc, J. J. & Rees, D. C. (1992). *Science*, **257**, 1653–1659.
- Gurman, S. J., Binsted, N. & Ross, I. (1984). *J. Phys. C*, **17**, 143–151.
- Hales, B. J., Case, E. E., Morningstar, J. E., Dzeda, M. F. & Maurer, L. A. (1986). *Biochemistry*, **25**, 7251–7255.
- Harvey, I., Arber, J. M., Eady, R. R., Smith, B. E., Garner, C. D. & Hasnain, S. S. (1990). *Biochem. J.* **266**, 929–931.
- Howard, J. B. & Rees, D. C. (1994). *Annu. Rev. Biochem.* **63**, 235–264.
- Kim, J. & Rees, D. C. (1992). *Science*, **257**, 1677–1682.
- Kim, J., Woo, D. & Rees, D. C. (1993). *Biochemistry*, **32**, 7104–7115.
- Mayer, S. M., Lawson, D. M., Gormal, C. A., Roe, S. M. & Smith, B. E. (1999). *J. Mol. Biol.* **292**, 871–891.
- Moore, V. G., Tittsworth, R. C. & Hales, B. J. (1994). *J. Am. Chem. Soc.* **116**, 12101–12102.
- Murphy, L. M., Strange, R. W., Karlsson, G., Lundberg, L., Pascher, T., Reinhammar, B. & Hasnain, S. S. (1993). *Biochemistry*, **32**, 1965–1975.
- Murshudov, G. N., Vagin, A. A. & Dodson, E. J. (1997). *Acta Cryst. D* **53**, 240–255.
- Schindelin, H., Kisker, C. & Rees, D. C. (1997). *J. Biol. Inorg. Chem.* **2**, 773–781.
- Smith, B. E., Eady, R. R., Lowe, D. J. & Gormal, C. (1988). *Biochem. J.* **250**, 299–302.

XAFS studies of nitrogenase: the MoFe and VFe proteins and the use of crystallographic coordinates in three-dimensional EXAFS data analysis. Erratum

Richard W. Strange,^{a*} Barry E. Smith,^b Robert R. Eady,^b David Lawson^b and S. Samar Hasnain^a

^aMolecular Biophysics Group, CCLRC Daresbury Laboratory, Warrington, Cheshire WA4 4AD, UK, and ^bDepartment of Biological Chemistry, John Innes Centre, Norwich NR4 7UH, UK. E-mail: r.w.strange@dl.ac.uk

One of the authors was omitted in the published version of the paper by Strange *et al.* [*J. Synchrotron Rad.* (2002), **10**, 71–75]. The full author list is given above. Since the acceptance of our paper, an atomic-resolution (1.16 Å) structure of MoFe-protein has emerged [Einsle *et al.* (2002), *Science*, **297**, 1696–1700]. We take this opportunity to update Table 1 of the paper, demonstrating improved agreement of the three-dimensional XAFS refinement with atomic-resolution metrical information.

Keywords: EXAFS; nitrogen fixation; nitrogenase; crystal structure; FeMoco.

Table 1

Constrained refinements of the Mo *K*-edge EXAFS using a three-dimensional refinement approach.

In the first refinement, distances are kept at crystallographic values and Debye–Waller (σ^2) values are refined; in the second refinement, the distances are also allowed to vary. A higher value than 0.03 Å² signifies that the atom is incorrectly placed and that little contribution to the EXAFS signal is made. ΔR is the difference in Mo–ligand distance from the crystallographic value averaged over the two independent $\alpha\beta$ units. The final column includes information from a 1.16 Å structure (Einsle *et al.*, 2002).

Ligand	First refinement		Second refinement		ΔR (Å)	1.16 Å structure (Å)
	<i>R</i> (Å)	σ^2 (Å ²)	<i>R</i> (Å)	σ^2 (Å ²)		
Mo–N(His)	2.48	0.11	2.29	0.003	–0.17	2.29
Mo–O5(homocitrate)	2.29	0.11	2.14	0.001	–0.16	2.18
Mo–O7(homocitrate)	2.35	0.11	2.31	0.001	–0.04	2.20
Mo–S1B	2.30	0.001	2.30	0.001	0.0	2.33
Mo–S3B	2.38	0.001	2.37	0.001	–0.01	2.37
Mo–S4B	2.35	0.001	2.35	0.001	0.00	2.33
Mo–Fe7	2.67	0.006	2.67	0.006	0.00	2.67
Mo–Fe6	2.68	0.006	2.67	0.006	–0.01	2.67
Mo–Fe5	2.71	0.006	2.71	0.006	0.00	2.73
Mo–Fe2	5.04	0.01	5.04	0.01	0.00	5.04
Mo–Fe3	5.06	0.01	5.06	0.01	0.00	5.05
Mo–Fe4	5.09	0.01	5.08	0.01	–0.01	5.10
Fit index		12.4		9.5		
<i>R</i> factor	46%		37%			

References

- Einsle, O., Tezcan, A., Andrade, S. L. A., Schmid, B., Yoshida, M., Howard, J. B. & Rees, D. C. (2002). *Science*, **297**, 1696–1700.
 Strange, R. W., Eady, R. R., Lawson, D. & Hasnain, S. S. (2003). *J. Synchrotron Rad.* **10**, 71–75.